Systematic comparison of numerical differentiators and an application to model-free control

Amine Othmane, Joachim Rudolph, Hugues Mounier

Version of Record: https://www.sciencedirect.com/science/article/pii/S0947358021000777
Manuscript_56388350ea45da8c1dfa06250b8282b1

Systematic comparison of numerical differentiators and an application to model-free control*

Amine Othmane[a,b,*], Joachim Rudolph[a] and Hugues Mounier[b]

[a]Chair of Systems Theory and Control Engineering, Saarland University, 66123 Saarbrücken, Germany
[b]Université Paris-Saclay, CNRS, CentraleSupélec, Laboratoire des signaux et systèmes, 91190, Gif-sur-Yvette, France

ARTICLE INFO

Keywords:
Numerical differentiation, Linear filtering, Orthogonal polynomials, Model-free control

ABSTRACT

Recent tuning guidelines for algebraic differentiators based on the analysis of the Fourier transform of the kernels are reviewed. A region of validity for the previous analyses carried out for high frequencies is proposed and the results are related to those based on the analysis of the $\mathcal{L}_2$-norm of the Fourier transform of the differentiators. These results are then used for a systematic comparison with established approaches from the literature (homogeneous, high-gain and sliding mode differentiators) for the estimation of the second derivative of a known signal corrupted by a known disturbance. It is shown that properly tuned and discretized algebraic differentiators outperform the other analyzed approaches in terms of robustness, convergence time, and tuning simplicity. The tuning guidelines are then used in the context of control of a partially known system, thus bridging the gap to the tuning of recent model-free control approaches.

1. Introduction

The importance of numerical differentiation, i.e., the derivative estimation of noisy time signals, is undeniable in many fields of engineering and applied mathematics. It is, however, a longstanding ill-posed and challenging problem. Many approaches have already been proposed, and only a few are named here. In the signal processing literature, the problem has been tackled using frequency-domain digital filter design techniques as in [4]. The control community has developed approaches based on observer design ([13, 5, 6, 14]) and differential algebraic methods ([19, 20]). This communication focuses on some of the approaches stemming from this community.

Starting from the early nineties, high-gain observers have been used in nonlinear control to estimate derivatives of the output and design output feedback control laws. The discrete-time implementation of high-gain (HG) observers and their use as numerical differentiators have been analyzed in [5] and [6]. In [29], an algorithm is presented to compute observer gains minimizing the estimation error bound. In [13] and [14], Levant uses sliding modes to design differentiators. It is shown in [18] that whereas the accuracy of the 1st-order sliding mode differentiator is preserved, the simplistic one-step Euler discretization destroys the accuracies of the higher-order sliding mode (HOSM) differentiators and proposes a new discretization scheme. Homogeneous (HO) finite-time differentiators have also been derived in [26]. The proposed approach unifies all the aforementioned observers into one single framework simplifying the comparison of estimation results. A totally different approach has been proposed in [19] and [20], where differential algebraic techniques have been used to derive differentiators. Later works ([11, 16]) have derived these estimators using approximation theoretic tools simplifying the analysis.

Some of the approaches have already been compared in the literature. The superiority of a third-order HG differentiator over a HOSM one has been shown in [29, 30]. In [2] HOSM differentiators yield better estimates than HG ones for a second-order system. However, simulations have shown in [17] that for a second order system HG differentiators outperform HOSM ones. Comparisons including algebraic differentiators (AD) can be found in [17, 30]. In [21] it has been shown that the AD has been improperly implemented in [30] and new comparison results have been presented proving the good performance of these differentiators. It is shown that they are more robust with respect to noise. However, the tuning of the differentiators is not explicitly provided in these publications.

Tuning guidelines for the AD have been developed in [11, 12, 22, 23]. In [11] an asymptotic analysis of the Fourier transform of the differentiator kernels has been proposed. In the current paper, the region of validity for the statement made in [11] is increased. This supports the proposed tuning guidelines and enables a comparison with the guidelines developed in [23]. Using these recent results, AD are then compared to the HOSM ([14]), HG ([6, 29]), and HO ([26]) ones for the estimation of the second derivative of a known signal corrupted by a known disturbance. Thus, all approaches can be designed according to the same signal model and be tuned using the necessary knowledge. The discretization of the approaches is also discussed due to its importance for practical implementations. The use of differentiators for the control of a partially known system is also analyzed. This part shows the application of the tuning guidelines in the context of model-free control ([9, 10]). Model-free control has been successfully applied in [3, 9, 10, 24].

*This work is supported by the "ADI 2018" project funded by the IDEX Paris-Saclay, ANR-11-IDEX-0003-0.
*Corresponding author
a.othmane@lsr.uni-saarland.de (A. Othmane);
j.rudolph@lsr.uni-saarland.de (J. Rudolph);
hugues.mounier@l2s.centralesupelec.fr (H. Mounier)
ORCID(s): 0000-0002-8871-3472 (A. Othmane); 0000-0002-0806-6106 (J. Rudolph)

However, the tuning of the estimators has not been discussed in any of these works and only the numerical values of the involved parameters have been reported. This work intends to fill this gap by using a case study to show how the latest results for the tuning of AD can be used for the design of model-free control algorithms and make them more accessible.

This work is structured as follows. The notation adopted in this work is introduced in Section 2, and algebraic differentiators are briefly recalled in Section 3. Tuning approaches based on the analysis of the Fourier transform of the differentiator are discussed therein. In Section 4, homogeneous, high-gain, and higher-order sliding mode differentiators are recalled in a unified framework. In Section 5.1, the tuning of algebraic differentiators is demonstrated in a simulation, and the estimation is compared to the other approaches. The control of a partially known system using numerical differentiation is illustrated in Section 5.2.

2. Notation

The $n \times n$, $n \in \mathbb{N}$, identity matrix is denoted I_n and the column vector with n zeros is denoted 0_n. The imaginary unit is denoted $\imath$, i.e., $\imath^2 = -1$. The gamma function ([1, Sec. 6.1]) is denoted Γ. Let $\alpha, \beta > -1$. The orthogonal Jacobi polynomial of degree $N \in \mathbb{N}$ ([1, Sec. 22.3]) associated with the weight function

$$w^{(\alpha,\beta)}(\tau) = \begin{cases} (1-\tau)^\alpha (1+\tau)^\beta, & \tau \in [-1,1], \\ 0, & \text{otherwise}, \end{cases}$$

is denoted $\mathrm{P}_N^{(\alpha,\beta)}$ and reads

$$\mathrm{P}_N^{(\alpha,\beta)}(\tau) = \sum_{k=0}^{N} \binom{N}{k} c_k^{(\alpha,\beta)} (\tau-1)^k,$$
$$c_k^{(\alpha,\beta)} = \frac{\Gamma(\alpha+N+1)\Gamma(\alpha+\beta+N+k+1)}{2^k N! \Gamma(\alpha+\beta+N+1)\Gamma(\alpha+k+1)},$$

for $\tau \in [-1,\ 1]$. Its zeros are denoted $p_{N,k}^{(\alpha,\beta)}$, $k \in \{1, \dots, N\}$, and their maximum is $p_N^{(\alpha,\beta)} = \max_k p_{N,k}^{(\alpha,\beta)}$.

3. Algebraic differentiators

3.1. Time-domain interpretation of algebraic differentiators

The algebraic numerical differentiation methods introduced in [19] and [20] have been initially derived using differential algebraic manipulations of truncated Taylor series. Later works ([11, 16]) have derived these differentiators using an approximation theoretical approach that yields a straightforward analysis of the estimate properties, especially the estimation delay. Assume $y : t \mapsto y(t)$ is a signal whose n-th derivative is Lebesgue integrable. The estimate of the n-th order derivative of y denoted $\hat{y}^{(n)}$ can be written as

$$\hat{y}^{(n)}(t) = \int_0^T \frac{\mathrm{d}^n}{\mathrm{d}\tau^n} g_{N,T,\vartheta}^{(\alpha,\beta)}(\tau)\, y(t-\tau)\mathrm{d}\tau, \tag{1}$$

with the filter kernel

$$g_{N,T,\vartheta}^{(\alpha,\beta)}(t) = \frac{2}{T} \sum_{i=0}^{N} \frac{\mathrm{P}_i^{(\alpha,\beta)}(\vartheta)}{\left\|\mathrm{P}_i^{(\alpha,\beta)}\right\|^2} w^{(\alpha,\beta)}(\nu(t))\, \mathrm{P}_i^{(\alpha,\beta)}(\nu(t)).$$

In the latter equation $\nu(t) = 1 - \frac{2}{T}t$, $\|x\| = \sqrt{\langle x, x\rangle}$ is the norm induced by the weighted inner product

$$\langle x, y\rangle = \int_{-1}^{1} w^{(\alpha,\beta)}(\tau) x(\tau) y(\tau)\mathrm{d}\tau,$$

N is the degree of the polynomial approximating the signal $y^{(n)}$ in the time window $[t-T, t]$, T is the filter window length, and ϑ parametrizes the estimation delay.

The attentive reader already recognizes the free parameters of the AD and the difficulty in the tuning process. The derivation of these filters using the approximation theoretical approach ([16, 11]) yields a condition $\alpha, \beta > n-1$ and an expression for the estimation delay

$$\delta_t = \begin{cases} \frac{\alpha+1}{\alpha+\beta+2} T, & \text{if } N = 0, \\ \frac{1-\vartheta}{2} T, & \text{otherwise}, \end{cases}$$

and the degree of exactness

$$\gamma = \begin{cases} n+N+1, & \text{if } N = 0 \vee \vartheta = p_{N+1,k}^{(\alpha,\beta)}, \\ n+N, & \text{otherwise}. \end{cases} \tag{2}$$

The degree of exactness was introduced in [11] as the polynomial degree up to which the derivative estimation is exact. If $\gamma = 2$ for example, the first and second time derivatives of a polynomial signal of degree two are exact up to a small known estimation delay. The effect of the parameters on the Fourier transform of $g_{N,T,\vartheta}^{(\alpha,\beta)}$ is analyzed in the sequel. This gives more insights into the robustness against disturbances.

3.2. Frequency-domain interpretation and tuning guidelines

For the tuning of the parameters, the frequency-domain interpretation has proven to be particularly effective. In [12, 22, 11, 23] different representations of the Fourier transform of a differentiator $g_{N,T,\vartheta}^{(\alpha,\beta)}$ have been derived. A possible representation is

$$\mathcal{G}_{N,T,\vartheta}^{(\alpha,\beta)}(\omega) = \mathrm{e}^{-\imath\omega T} \sum_{i=0}^{N} b_i \sum_{k=0}^{i} c_{i,k} \widetilde{\mathrm{M}}_{i,k}^{(\alpha,\beta)}(\imath\omega T)$$

with

$$b_i = \frac{\alpha+\beta+2i+1}{\alpha+\beta+i+1} \mathrm{P}_i^{(\alpha,\beta)}(\vartheta),$$
$$c_{i,k} = (-1)^{i-k} \binom{i}{k},$$
$$\widetilde{\mathrm{M}}_{i,k}^{(\alpha,\beta)}(\imath\omega T) = \mathrm{M}(\alpha+k+1, \alpha+\beta+i+2, \imath\omega T),$$

where M is the confluent hypergeometric function of the first kind described in [1, Sec. 13.1]. In the sequel, the analysis is

restricted to the case $\beta \geqslant \alpha$. Exchanging α and β, and mirroring the estimation delay at $T/2$ yields the identical amplitude spectrum. Thus, using these symmetry properties of $g_{N,T,\vartheta}^{(\alpha,\beta)}$, the results of this Section also hold for $\alpha < \beta$. The analysis is further restricted to the special case $\vartheta > p_N^{(\alpha,\beta)}$ which, due to the properties of the Jacobi polynomials ([28, Sec. 3.3]), incorporates the special cases $\vartheta \in \left\{1, p_{N+1}^{(\alpha,\beta)}\right\}$. While in the first case the estimation delay is zero, it is minimized in the second case and the degree of exactness is increased by one.

Using the developments from Appendix A and some computations omitted for brevity, it follows for all $|\omega| \geqslant |\alpha - \beta + N|/T = \omega_0$ that

$$\mathcal{G}_{N,T,\vartheta}^{(\alpha,\beta)}(\omega) = \mathcal{F}_{N,T,\vartheta}^{(\alpha,\beta)}(\omega) + \mathcal{H}(\omega)$$

with $|\mathcal{H}(\omega)| = \mathcal{O}\left(|\omega|^{-\alpha-2}\right)$, the quantities

$$\begin{aligned}
\mathcal{F}_{N,T,\vartheta}^{(\alpha,\beta)}(\omega) &= \left(\frac{r_{N,\vartheta}^{(\mu,\kappa)}}{(\omega T)^{\mu}} \mathrm{e}^{\imath\frac{1}{2}\phi(\omega T)} \right. \\
&\quad \left. + \frac{s_{N,\vartheta}^{(\mu,\kappa)}}{(\omega T)^{\mu+\kappa}} \mathrm{e}^{-\imath\frac{1}{2}\phi(\omega T)}\right) \mathrm{e}^{\frac{\imath}{2}\left(\pi\frac{\kappa}{2}-\omega T\right)} \\
\phi(\omega) &= \omega - \pi\left(\mu + \frac{\kappa}{2}\right), \\
r_{N,\vartheta}^{(\mu,\kappa)} &= \sum_{i=0}^{N} \frac{c_i^{(\mu,\kappa)}}{\Gamma(\mu+\kappa+i)} \mathrm{P}_i^{(\mu-1,\mu+\kappa-1)}(\vartheta), \\
s_{N,\vartheta}^{(\mu,\kappa)} &= \sum_{i=0}^{N} (-1)^i \frac{c_i^{(\mu,\kappa)}}{\Gamma(\mu+i)} \mathrm{P}_i^{(\mu-1,\mu+\kappa-1)}(\vartheta), \\
c_i^{(\mu,\kappa)} &= (2\mu+\kappa+2i-1)\,\Gamma(2\mu+\kappa+i-1),
\end{aligned}$$

and the constants $\mu = 1 + \min\{\beta, \alpha\}$ and $\kappa = |\beta - \alpha|$. An explicit formulation for $\mathcal{H}$ is omitted for lack of space. This approximation has also been derived in [11] for $\omega \to \infty$. The current work gives an explicit region of validity $\mathcal{V}_{\mathcal{G}_{N,T,\vartheta}^{(\alpha,\beta)}} = \mathbb{R} \setminus (-\omega_0, \omega_0)$ for these results so that the approximations can be rigorously used to simplify the analysis of the effects of the filter parameters for all $\omega \in \mathcal{V}_{\mathcal{G}_{N,T,\vartheta}^{(\alpha,\beta)}}$. Also, the developed tuning guidelines become more informative. The size of $\mathcal{V}_{\mathcal{G}_{N,T,\vartheta}^{(\alpha,\beta)}}$ increases with increasing parameters T and β and decreasing parameters N and α.

The function $\mathcal{F}_{N,T,\vartheta}^{(\alpha,\beta)}$ is analyzed in the sequel where it is considered an approximation of $\mathcal{G}_{N,T,\vartheta}^{(\alpha,\beta)}$ in $\mathcal{V}_{\mathcal{G}_{N,T,\vartheta}^{(\alpha,\beta)}}$ with the approximation error $\mathcal{H}$. It satisfies

$$\underline{\mathcal{F}}_{N,T,\vartheta}^{(\alpha,\beta)}(\omega) \leqslant \left|\mathcal{F}_{N,T,\vartheta}^{(\alpha,\beta)}(\omega)\right| \leqslant \overline{\mathcal{F}}_{N,T,\vartheta}^{(\alpha,\beta)}(\omega),$$

for all $\omega \in \mathbb{R} \setminus \{0\}$ with the lower and upper bounds

$$\begin{aligned}
\underline{\mathcal{F}}_{N,T,\vartheta}^{(\alpha,\beta)}(\omega) &= \left|\left|\frac{r_{N,\vartheta}^{(\mu,\kappa)}}{(\omega T)^{\mu}}\right| - \left|\frac{s_{N,\vartheta}^{(\mu,\kappa)}}{(\omega T)^{\mu+\kappa}}\right|\right|, \\
\overline{\mathcal{F}}_{N,T,\vartheta}^{(\alpha,\beta)}(\omega) &= \left|\frac{r_{N,\vartheta}^{(\mu,\kappa)}}{(\omega T)^{\mu}}\right| + \left|\frac{s_{N,\vartheta}^{(\mu,\kappa)}}{(\omega T)^{\mu+\kappa}}\right|.
\end{aligned}$$

The effects of the different parameters on $\mathcal{F}_{N,T,\vartheta}^{(\alpha,\beta)}$ are analyzed and compared with the developments in [23].

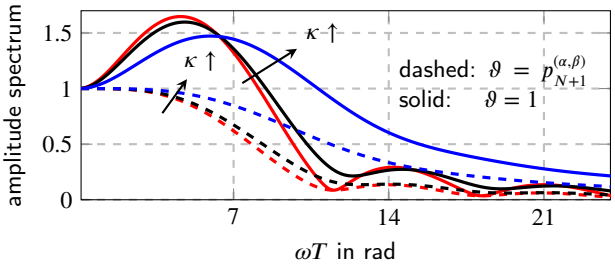

Figure 1: Variation of the amplitude with respect to the normalized frequency with $\kappa \in \{0, 0.5, 2\}$, $\mu = 1$, and $N = 1$.

3.2.1. *Effect of* N

The attention is first focused on the parameter N and the function

$$\delta\mathcal{F}_{N,T,\vartheta}^{(\alpha,\beta)} = \left(\overline{\mathcal{F}}_{N,T,\vartheta}^{(\alpha,\beta)} + \underline{\mathcal{F}}_{N,T,\vartheta}^{(\alpha,\beta)}\right)/2,$$

which can be seen as an approximation of the filter. For sufficiently large ω this function satisfies

$$\delta\mathcal{F}_{N,T,\vartheta}^{(\alpha,\beta)}(\omega) = \max\left\{\left|\frac{r_{N,\vartheta}^{(\mu,\kappa)}}{(\omega T)^{\mu}}\right|, \left|\frac{s_{N,\vartheta}^{(\mu,\kappa)}}{(\omega T)^{\mu+\kappa}}\right|\right\} = \left|\frac{r_{N,\vartheta}^{(\mu,\kappa)}}{(\omega T)^{\mu}}\right|, \quad (4)$$

where the properties of the Jacobi polynomials ([28, Sec. 3.3]) are used for the simplification.

Let N and $\bar{N}$ be two natural numbers satisfying $\bar{N} > N$. Let ϑ_N and $\vartheta_{\bar{N}}$ be two scalars satisfying $\vartheta_N > p_N^{(\alpha,\beta)}$ and $\vartheta_{\bar{N}} > p_{\bar{N}}^{(\alpha,\beta)}$. Then, $\left|r_{N,\vartheta_N}^{(\mu,\kappa)}\right| < \left|r_{\bar{N},\vartheta_{\bar{N}}}^{(\mu,\kappa)}\right|$. Thus, for sufficiently large ω the value of $\delta\mathcal{F}_{N,T,\vartheta}^{(\alpha,\beta)}(\omega)$ decreases with decreasing N, i.e., additive high frequency disturbances are better attenuated the smaller N is. This analysis supports the results of [23, Prop. 3.1] proving that the $\mathcal{L}_2$-norm $\left\|\mathcal{G}_{N,T,\vartheta}^{(\alpha,\beta)}\right\|_{\mathcal{L}_2}$ increases with increasing parameter N.

3.2.2. *Effect of* ϑ

From (2) it was already clear that the choice $\vartheta = p_{N+1,k}^{(\alpha,\beta)}$ increases the degree of exactness. For $\bar{\vartheta} \geqslant \vartheta = p_{N+1}^{(\alpha,\beta)} \neq 1$ it can also be observed that $\left|r_{N,\vartheta}^{(\mu,\kappa)}\right| \leqslant \left|r_{N,\bar{\vartheta}}^{(\mu,\kappa)}\right|$. It follows that $\delta\mathcal{F}_{N,T,\vartheta}^{(\alpha,\beta)}$ increases with increasing ϑ. So, for the delay-free estimation not only the degree of exactness is reduced, but the filter is less robust against disturbances as depicted in Fig. 1.

3.2.3. *Effect of* α *and* β

From (4) it is clear that $\mu = 1 + \alpha$ characterizes the order of the low pass filter, which is an early result from [12]. However, attention is required. From [28, Thm. 6.21.1] it is known that $\frac{\mathrm{d}p}{\mathrm{d}\alpha}(\alpha) < 0$, with $p(\alpha) = p_{N+1,k}^{(\alpha,\beta)}$, i.e., for $\vartheta = p_{N+1}^{(\alpha,\beta)}$ the estimation delay increases with increasing α.

It was shown in [11, Sec. 3.3.2] that for a sought cutoff frequency of the filters the choice $N = 0$ and $\alpha = \beta$ yields the smallest T and, thus, a reduced estimation error.

For the effect on additive high frequency disturbances, the quantity $\Delta\mathcal{F}_{N,T,\vartheta}^{(\alpha,\beta)} = \overline{\mathcal{F}}_{N,T,\vartheta}^{(\alpha,\beta)} - \underline{\mathcal{F}}_{N,T,\vartheta}^{(\alpha,\beta)}$, introduced in [11,

Sec. 3.3.3] and which is for sufficient large ω proportional to $\omega^{-\mu-\kappa}$, can be analyzed. Increasing $\kappa = \beta - \alpha$ yields a faster decrease of the stopband ripple that enhances the disturbance attenuation. This illustrates the results from [23, Prop. 3.1 and Lem. 3.2] showing that the overall output noise power increases with increasing κ. Again, attention is required for the case $\vartheta = 1$, i.e., for delay-free estimations, where the amplitude of $\mathcal{G}_{N,T,\vartheta}^{(\alpha,\beta)}$ exhibits overshoots (see Fig. 1) which decrease with increasing κ.

3.3. Discretization

In [19, 20] the AD are discretized using the trapezoidal rule. However, using the mid-point rule, a discrete implementation requires one filter value less and reduces the estimation delay by half of the sampling period t_s. It is assumed that the filter window length is a multiple of the sampling period t_s. At the i-th step, the estimate in (1) becomes

$$\hat{y}^{(n)}\left(it_s + \frac{1}{2}\right) = \frac{1}{\Phi}\sum_{k=0}^{L_g-1} w\left(k, t_s\right) y\left((i-k)t_s\right)$$

with the filter length $L_g = T/t_s$, the weights

$$w(k, t_s) = \frac{\mathrm{d}^n}{\mathrm{d}t^n} g_{N,T,\vartheta}^{(\alpha,\beta)}(t)\Big|_{t=(k+1/2)t_s},\ k = 0, \ldots, L_g - 1,$$

and

$$\Phi = \frac{t_s^n}{n!}\sum_{k=0}^{L_g-1} w^n(-k, t_s).$$

The constant Φ is a normalization factor that takes the discretization error into account. For an in-depth analysis, the reader is referred to the detailed investigations in [11, Ch. 3].

4. Continuous finite-time differentiators

Consider a smooth signal $y : t \mapsto y(t)$ whose derivatives up to the order $n-1$, $n \in \mathbb{N}$, have to be estimated. Assume further that $y^{(n)}(t) = \theta\left(\dot{y}(t), \ldots, y^{(n-1)}(t)\right)$. Let

$$x(t) = \begin{bmatrix} y(t) & \dot{y}(t) & \ldots & y^{(n-1)}(t) \end{bmatrix}^{\mathrm{T}} \in \mathbb{R}^n.$$

Then,

$$\begin{aligned} \dot{x}(t) &= \begin{bmatrix} 0_{n-1} & I_{n-1} \\ & 0_n^{\mathrm{T}} \end{bmatrix} x(t) + \begin{bmatrix} 0_{n-1} \\ 1 \end{bmatrix} \theta(t), \\ y(t) &= \begin{bmatrix} 1 & 0_{n-1} \end{bmatrix} x(t). \end{aligned}$$

Perruquetti and Floquet ([26]) propose the following homogeneous differentiator

$$\begin{aligned} \dot{\hat{x}}_i(t) &= \hat{x}_{i+1}(t) - k_i \lfloor \hat{x}_1(t) - y(t) \rceil^{i\nu-(i-1)}, \\ \dot{\hat{x}}_n(t) &= -k_n \lfloor \hat{x}_1(t) - y(t) \rceil^{n\nu-(n-1)}, \end{aligned} \tag{5}$$

where $i = 1, \ldots, n-1$, $\lambda \mapsto \lambda^n + \sum_{i=1}^n k_i \lambda^{n-i}$ is a Hurwitz polynomial, $\nu \in \left(\frac{n-1}{n}, 1\right)$, the function

$$\lfloor z \rceil^{\nu} = \mathrm{sign}(z)\,|z|^{\nu}, \quad z \in \mathbb{R},$$

and $\hat{x}(t_0) = \hat{x}_0 \in \mathbb{R}^n$, $t_0 \in \mathbb{R}$. As mentioned in [26] it is impossible to obtain the convergence of the estimation error $e(t) = x(t) - \hat{x}(t)$ to zero without any additional information about θ. To overcome this problem, it can be assumed that y is locally polynomial on a small time interval, i.e., $y^{(n)}(t) = \theta\left(\dot{y}(t), \ldots, y^{(n-1)}(t)\right) = 0$, and in that case, it is possible to recover the time derivative. Otherwise, it can be assumed that θ is bounded, i.e., there exists an $L \in \mathbb{R}$ such that $\left|y^{(n)}(t)\right| \leqslant L$ for all t. Thus, the function θ needs to be dominated by a discontinuous output injection as proposed in [26], for example.

4.1. Link with high-gain differentiators

The limit case $\nu = 1$ corresponds to the well-known Luenberger observer. If the parameters k_i, $i \in \{1, \ldots, n\}$, are chosen such that $k_i = \bar{k}_i/\epsilon^i$, with $\epsilon \ll 1$ and

$$\lambda \mapsto \lambda^n + \sum_{i=1}^n \bar{k}_i \lambda^{n-i}$$

a Hurwitz polynomial, the high-gain differentiators developed in [6] are recovered. In [7] it is shown using singular perturbation analysis that the estimation error will decay to $\mathcal{O}(\epsilon)$ after an unknown transient time period $[0,\ T_1(\epsilon)]$ where $\lim_{\epsilon\to 0} T_1(\epsilon) = 0$.

In the presence of a uniformly bounded disturbance η, the investigations in [29] prove that the ultimate bound on the estimation error for the k-th derivative, $1 \leqslant k \leqslant n-1$, is $\delta + P_{k+1}\left\|y^{(n)}\right\|_\infty + Q_{k+1}\|\eta\|_\infty / \epsilon^k$, for δ an arbitrary small constant, and P_{k+1} and Q_{k+1} scalars depending on all the differentiator parameters k_i. Note that this bound does not take into account the low pass characteristic of these differentiators. Tuning guidelines for ϵ are proposed in [29]. Dabroom and Khalil show in [6] that the bilinear transformation method gives the best performance for the discrete-time implementation.

4.2. Link with higher-order sliding mode differentiators

Letting ν approach $1 - 1/n$ yields $\lfloor x \rceil^{\nu} \to \mathrm{sign}(x)$. For $\nu = 1 - 1/n$ the differentiator in (5) becomes

$$\begin{aligned} \dot{\hat{x}}_i(t) &= \hat{x}_{i+1}(t) - k_i \left|\hat{x}_1(t) - y(t)\right|^{\frac{n-i}{n}} \mathrm{sign}\left(\hat{x}_1(t) - y(t)\right), \\ \dot{\hat{x}}_n(t) &= -k_n \mathrm{sign}\left(\hat{x}_1(t) - y(t)\right), \end{aligned} \tag{6}$$

where $i = 1, \ldots, n-1$, which corresponds to the $(n-1)$-th robust exact differentiator with finite-time convergence proposed in [14]. If the parameters k_i, $i = 1, \ldots, n$, are properly chosen, the estimation error reaches zero after a finite transient time. From [14, Thm. 6] it follows that the k-th order differentiator provides a much better accuracy of the l-th order derivative for $l < k$, than the l-th order differentiator.

Letting $k_i = \bar{k}_i L^{1/(n-i+1)}$ in (6) , with $\bar{k}_i$ properly chosen (see [18] and [14] for more details) and $L > 0$ the Lipschitz constant of the $(n-1)$-th derivative of y, the estimation error

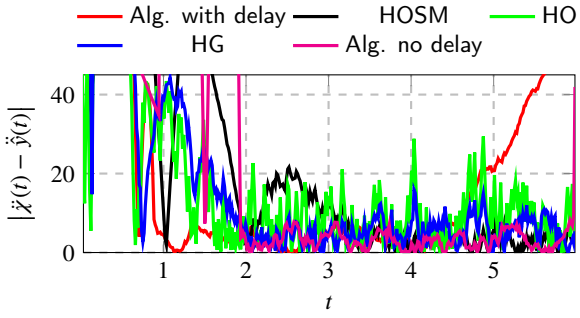

Figure 2: Estimation errors of the 2-nd derivative of a polynomial signal for different differentiators.

in the presence of a Lebesgue-measurable disturbance with magnitude not exceeding $\eta_{\max}$, yields the error

$$\left|\hat{x}_i(t) - y^{(i-1)}(t)\right| = \mathcal{O}\left(\eta_{\max}^{(n-i+1)/(n+1)}\right).$$

A popular choice for the parameters when $n \leqslant 6$ is $\bar{k}_1 = 1.1$, $\bar{k}_2 = 1.5$, $\bar{k}_3 = 3$, $\bar{k}_4 = 5$, $\bar{k}_5 = 8$ and $\bar{k}_6 = 12$ (see [15, 27, 18] for more details).

The discrete-time implementation of this differentiator is studied in [18] where a discretization scheme, which preserves the ultimate accuracy of the continuous-time HOSM differentiator also with discrete measurements, is proposed.

5. Simulation Results

5.1. Polynomial signals

The second derivative of a signal

$$\chi : t \mapsto \chi(t) = \sum_{i=0}^{4} a_i t^i,$$

where $a_0 = 13$, $a_1 = -60$, $a_2 = 46$, $a_3 = -12$ and $a_4 = 1$, will be estimated. The measurement is $y = \chi + \eta$, where η is a zero mean white noise. The signal-to-noise ratio (SNR) is equal to 31 dB. To compare the estimation results, the SNR for a differentiator, computed after its transient time, is defined as

$$\frac{\sum_{i=0}^{N_s} \ddot{y}^2(t_i)}{\sum_{i=0}^{N_s} \left(\ddot{\hat{y}}(t_i) - \ddot{\chi}(t_i)\right)^2}, \tag{7}$$

with N_s the total number of samples, $\ddot{\hat{y}}$ the estimate of $\ddot{y}$, and $\ddot{\hat{\chi}}$ the estimate of $\ddot{\chi}$. All differentiators are designed to meet the model of the signal so that the estimation error stems solely from the noise. Thus, the robustness to noise can be analyzed.

5.1.1. *Parametrization of algebraic differentiators*

Based on the investigations in Section 3.2, the parameters α and β are chosen equal. For the filter to be a differentiator, these parameters have to satisfy $\alpha, \beta > 1$. Since the signal is known, the cutoff frequency of the filter can be chosen. Two algebraic differentiators (with and without delay) with the cutoff frequency $\omega_c = 7$, the degree of exactness $\gamma = 4$ and $\alpha = \beta = 2$ are designed.

Table 1
The SNR in dB of the differentiators

	Alg. del.	Alg. no del.	HOSM	HG	HO
SNR	20.21	24.89	19.98	20.51	11.94

5.1.2. *Parametrization of HOSM differentiators*

The order of the differentiator is three. Since the signal in known, the HOSM (6) can be parameterized by $k_i = \bar{k}_i L^{1/(n-i+1)}$, with L the Lipschitz constant of $\chi^{(4)}$ and $\bar{k}_i$ taking the aforementioned values.

5.1.3. *Parametrization of HG differentiators*

Since the noise and the signal are perfectly known, the HG differentiator in (5) with $\nu = 1$ is tuned following the guidelines in [29]. The order of the differentiator is four. The observer poles are chosen at -2, -5, -8 and -10. The low pass behavior of the observer is comparable to that of the AD.

5.1.4. *Parametrization of HO differentiators*

For the results to be comparable, the parameters k_i in (5) are the same as for the HG differentiator and $\nu = 0.8$.

5.1.5. *Results*

All differentiators are discretized using the approaches discussed above, with a discretization step $t_s = 0.015$, and all observers are initialized at zero.

The SNR of the differentiators defined in (7) are summarized in Table 1 where it can be seen that the HO has the worst noise rejection properties, which has already been observed in [30], where a polynomial fit in a sliding window had to be used to decrease the noise effects. The delayed estimate from the AD is the most robust against the disturbances. The remaining approaches show similar SNR values. Comparing the results of the two AD confirms the observation in Section 3.2 that accepting a delay increases the robustness against noise. The estimation results are depicted in Fig. 2. From the results it is clear that the AD converge the fastest (with a precisely known convergence time equal to T). The delayed AD depicts the biggest error. However, this is due to the (known) delay, which, in specific applications can be compensated by appropriately combining the differentiator with a predictor or an observer.

Furthermore, the tuning of the HG, HOSM and HO differentiators necessitated considerable information on the unknown derivatives of the signal and the disturbance, which is delicate for unknown signals. In the modest opinion of the authors, the proposed analysis in Section 3, the interpretation of the AD as finite impulse response filters and the rich results for the design of such filters developed in the literature facilitates the construction of differentiators. In addition, the only requirement on the sought derivative is its Lebesgue integrability. Moreover, *optimal* filters can be designed for every individual needed derivative which is not possible using a single observer. The optimal parameters for the HG for estimating the first derivative will differ from

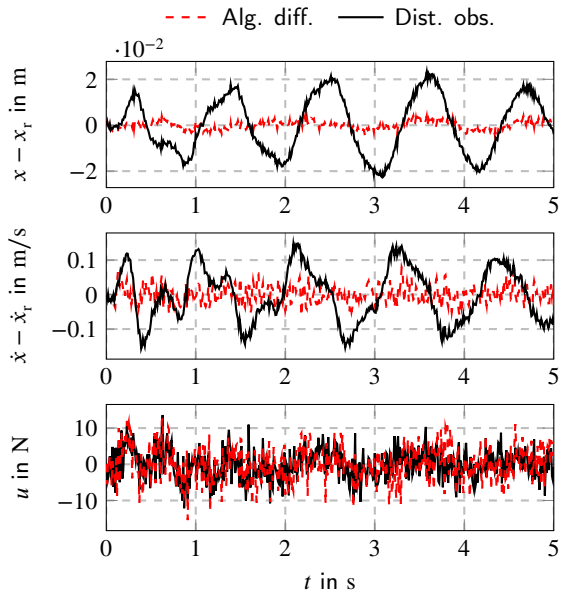

Figure 3: Time evolution of errors and input.

the optimal choice for estimating the second derivative, for example, and an averaging of the parameters is proposed in [29].

5.2. Control application

5.2.1. System analysis

Consider the model of a cart ([8, Ex. 3.10]), with position x and mass m_1, and an attached mathematical pendulum, whose angle with respect to the vertical is θ, length is l and mass is m_2. For notational convenience the explicit dependence on time is omitted. With the gravity denoted g, the dynamics are

$$\begin{aligned}\left(m_1 + m_2\right)\ddot{x} + m_2 l\left(\ddot{\theta}\cos(\theta) - \dot{\theta}^2\sin(\theta)\right) &= u,\\ m_2\left(l^2\ddot{\theta} + l\ddot{x}\cos(\theta)\right) - m_2 g l\sin(\theta) &= 0,\end{aligned}$$

with u the force applied to the cart. A measurement $y = x$ is available.

Controlling the position of the car without any knowledge of the pendulum dynamics is considered. Denote the force of the pendulum acting on the cart as F_p. It satisfies

$$F_\mathrm{p} = m_2\ddot{x} + m_2 l\left(\ddot{\theta}\cos(\theta) - \dot{\theta}\sin(\theta)\right),$$

which is considered as unknown in this work. The interesting dynamics are

$$m_1\ddot{x} + F_\mathrm{p} = u. \tag{9}$$

Let $\hat{F}_\mathrm{p}$ be an estimate of F_p and x_r a sufficiently smooth reference trajectory. The controller

$$u = m_1\ddot{x}_\mathrm{r} + \hat{F}_\mathrm{p} + k_\mathrm{p}(x - x_\mathrm{r}) + k_\mathrm{d}(\dot{x} - \dot{x}_\mathrm{r}), \quad k_\mathrm{p}, k_\mathrm{d} < 0,$$

is considered. For the estimation of F_p the ansatz

$$\begin{aligned}\dot{z}_1 &= z_2 + l_1(z_1 - y), \quad z_1(0) = z_{10},\\ \dot{z}_2 &= \frac{u}{m_1} + l_2(z_1 - y), \quad z_2(0) = z_{20},\end{aligned}$$

with $l_1, l_2 > 0$ of a linear observer is considered. One can easily show that $F_\mathrm{p} = m_1\left(-\ddot{e} + l_1\dot{e} + l_2 e\right)$, with $e = y - z_1$.

Using the discussed differentiation techniques one can write

$$\hat{F}_\mathrm{p} = m_1\left(-\ddot{\hat{e}} + l_1\dot{\hat{e}} + l_2\hat{e}\right), \tag{10}$$

where the quantities with a hat denote estimated ones. In the simulation the measurement y is corrupted by a white Gaussian noise with mean zero and standard deviation σ.

Before discussing the simulation results, a look to established methods in the literature of model-free control especially in [9, 10] and their relations to the current one is necessary. In fact (9) is a special case of the *ultra-local model* introduced in [10, Eq. (1)]. Equation (10) evaluated at $t - \delta$, with $\delta > 0$, and the choice $l_1 = l_2 = 0$ yields $\hat{F}_\mathrm{p}(t) = -m_1\ddot{y}(t-\delta) + u(t-\delta)$ which corresponds to the work developed in [9]. For lack of space, the relation to the approach in [10] is not analyzed.

5.2.2. Simulation results

The initial values in (8) are $x(0) = \dot{x}(0) = 0$, $\theta(0) = -\pi/3\,\mathrm{rad}$ and $\dot{\theta}(0) = -\pi/3\,\mathrm{rad\,s^{-1}}$. The numerical values of the system parameters are $m_1 = 1\,\mathrm{kg}$, $m_2 = 0.25\,\mathrm{kg}$, $g = 9.81\,\mathrm{m\,s^{-2}}$, and $l = 0.25\,\mathrm{m}$. For the measurement noise $\sigma = 1\,\mathrm{mm}$. The reference trajectory x_r is a polynomial of degree five that enables a transition from 0 m to 0.7 m in 1.7 s and its time evolution is given in Fig. 4 by the blue dash-dotted curve.

Three delay-free algebraic differentiators with a cut-off frequency $\omega_c = 80\,\mathrm{rad\,s^{-1}}$, amplitudes falling with 20 dB per decade for high frequencies, and the parameter N equal to one are used in (10). The analysis of the first Section yields the numerical values of the different parameters. The controller gains are $k_\mathrm{p} = -20\,\mathrm{N\,m^{-1}}$ and $k_\mathrm{d} = -1.5\,\mathrm{N\,s\,m^{-1}}$. The gains for the observer are $l_1 = 200\,\mathrm{s^{-1}}$ and $l_2 = 10\times 10^4\,\mathrm{s^{-2}}$.

As a comparison the same controller is implemented when the force F_p is estimated by a linear disturbance observer for the system (9) with the assumption that $\dot{F}_\mathrm{p} \approx 0$. The observer poles lie at $-120\,\mathrm{s^{-1}}$.

The estimation algorithms and the controllers are implemented with a discretization step $t_s = 1\,\mathrm{ms}$. All observers are implemented using Euler forward and initialized at zero. Figures 3 and 4 show the promising results of the approach using algebraic differentiators.

6. Conclusion

In this work, recent frequency-domain tuning approaches for algebraic differentiators have been reviewed and compared. The first approach is based on the asymptotic approximation of the Kummer M function, which appears in the Fourier transform of the filter kernel. A region of validity for the approximation of the amplitude of the Fourier transform of the filter has been proposed. The second approach is based on the analysis of the $\mathcal{L}_2$-norm of the filter amplitude.

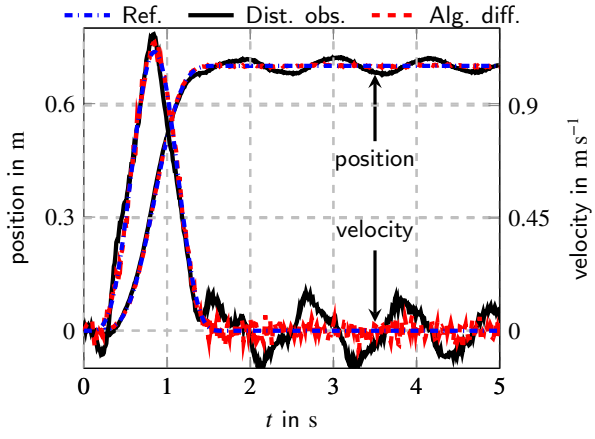

Figure 4: Time evolution of position and velocity.

The rich results for the design of finite impulse response filters developed in the literature in combination with the analysis of the algebraic differentiators facilitate their systematic tuning.

These systematic tuning guidelines have then been used to design algebraic differentiators and compare the estimation results with established algorithms from the literature, such as homogeneous, high-gain, and sliding mode differentiators. All differentiators have been designed to meet the model of the signal so that the robustness with respect to additive noise can be analyzed in detail. In the modest opinion of the authors, using the presented tuning approaches of the algebraic differentiators permits a more accessible and more systematic design of robust differentiators.

Finally, the presented tuning guidelines have been applied in a case study for the design of differentiators to control a partially known system. This is an attempt to propose tuning guidelines for the recently proposed model-free controllers in [10, 9] and make these approaches accessible to a broader audience.

A. Approximation of the Kummer M function

A solution to Kummer's differential equation ([1, Sec. 13.1]) is

$$\mathrm{M}(a,b,z) = \sum_{s=0}^{\infty} \frac{(a)_s}{\Gamma(b+s)\,s!} z^s, \quad a,b \in \mathbb{R} \text{ and } z \in \mathbb{C},$$

with $(a)_s$ the Pochhammer symbol. This function can be rewritten for all $a, b \in \mathbb{R}$ and $z \in \mathbb{C}$ as

$$\begin{aligned}\mathrm{M}(a,b,z) = {} & \gamma_{b,\delta} \mathrm{e}^{\mp a\pi\imath} \mathrm{U}^{(a,b)}(z) + \\ & + \gamma_{b,a} \mathrm{e}^{\pm\delta\pi\imath + z} \mathrm{U}^{(\delta,b)}\left(\mathrm{e}^{\pm\pi\imath} z\right)\end{aligned}$$

with $\delta = b - a$, $\gamma_{a,b} = \frac{\Gamma(a)}{\Gamma(b)}$ and the function U satisfying

$$\mathrm{U}^{(a,b)}(z) = z^{-a} \sum_{s=0}^{n-1} \frac{(a)_s (-\delta+1)_s}{s!} (-z)^{-s} + \epsilon_n(a,b,z).$$

The function ϵ_n is the error when U is approximated by the later series. In the sequel z is assumed to be purely imaginary with $|z| \geqslant |b-2a|$. From [25] it follows that ϵ_n satisfies

$$\left|\epsilon_n(a,b,z)\right| \leqslant 2\alpha\chi(n) \left|\frac{(a)_n(\delta+1)_n}{n!z^{a+n}}\right| \mathrm{e}^{\frac{2\alpha\rho\chi(1)}{|z|}} =: \epsilon_n^+(a,b,z)$$

with

$$\chi(n) = \sqrt{\pi}\frac{\Gamma\left(\frac{1}{2}n+1\right)}{\Gamma\left(\frac{1}{2}(n+1)\right)}, \qquad \alpha = \frac{1}{1-\sigma},$$

$$\rho = \frac{1}{2}\left|2a^2 - 2ab + b\right| + \frac{\sigma\left(1+\frac{1}{4}\sigma\right)}{(1-\sigma)^2}, \quad \sigma = \left|\frac{b-2a}{z}\right|.$$

Thus, for $n = 1$ the function M can be approximated as

$$\mathrm{M}(a,b,z) = \gamma_{b,\delta}\mathrm{e}^{a\pi\imath} z^{-a} + \gamma_{b,a}\mathrm{e}^{z} z^{-\delta} + \Delta_1(a,b,z).$$

with

$$\left|\Delta_1(a,b,z)\right| \leqslant \left|\gamma_{b,\delta}\right| \epsilon_1^+(a,b,z) + \left|\gamma_{b,a}\right| \epsilon_1^+(\delta,a,\mathrm{e}^{\pm\pi\imath} z).$$

References

[1] Abramowitz, M., Stegun, I.A. (Eds.), 1964. Handbook of Mathematical Functions with Formulas, Graphs, and Mathematical Tables. Dover, New York.

[2] Ahmed, H., Ríos, H., Ayalew, B., Wang, Y., 2018. Second-order sliding-mode differentiators: an experimental comparative analysis using Van der Pol oscillator. Int. J. Control 91, 2100–2112.

[3] Andary, S., Chemori, A., Benoit, M., Sallantin, J., 2012. A dual model-free control of underactuated mechanical systems, application to the inertia wheel inverted pendulum, in: 2012 American Control Conf., pp. 1029–1034.

[4] Chen, C.K., Lee, J.H., 1995. Design of high-order digital differentiators using L_1 error criteria. IEEE Trans. Circuits Syst. II. Analog Digit. Signal Process. 42, 287–291.

[5] Dabroom, A.M., Khalil, H.K., 1997. Numerical differentiation using high-gain observers, in: Proc. 36th IEEE Conf. on Decision and Control, pp. 4790–4795.

[6] Dabroom, A.M., Khalil, H.K., 1999. Discrete-time implementation of high-gain observers for numerical differentiation. Int. J. Control. 72, 1523–1537.

[7] Esfandiari, F., Khalil, H.K., 1992. Output feedback stabilization of fully linearizable systems. Int. J. Control 56, 1007–1037.

[8] Fabien, B.C., 2008. Analytical System Dynamics: Modeling and Simulation. Springer US.

[9] Fliess, M., Join, C., 2009. Model-free control and intelligent PID controllers: Towards a possible trivialization of nonlinear control? IFAC Proc. Volumes 42, 1531 – 1550.

[10] Fliess, M., Join, C., 2013. Model-free control. Int. J. Control 86, 2228–2252.

[11] Kiltz, L., 2017. Algebraische Ableitungsschätzer in Theorie und Anwendung. PhD dissertation. Saarland University.

[12] Kiltz, L., Rudolph, J., 2013. Parametrization of algebraic numerical differentiators to achieve desired filter characteristics, in: Proc. 52nd IEEE Conf. on Decision and Control, pp. 7010–7015.

[13] Levant, A., 1998. Robust exact differentiation via sliding mode technique. Automatica 34, 379 – 384.

[14] Levant, A., 2003. Higher-order sliding modes, differentiation and output-feedback control. Int. J. Control 76, 924–941.

[15] Levant, A., 2005. Quasi-continuous high-order sliding-mode controllers. IEEE Trans. Autom. Control 50, 1812–1816.

[16] Liu, D.Y., Gibaru, O., Perruquetti, W., 2011. Differentiation by integration with Jacobi polynomials. J. Comput. Appl. Math. 235, 3015 – 3032.

[17] Liu, D.Y., Gibaru, O., Perruquetti, W., 2014. Synthesis on a class of algebraic differentiators and application to nonlinear observation, in: Proc. 33rd Chinese Control Conf., pp. 2592–2599.

[18] Livne, M., Levant, A., 2014. Proper discretization of homogeneous differentiators. Automatica 50, 2007 – 2014.

[19] Mboup, M., Join, C., Fliess, M., 2007. A revised look at numerical differentiation with an application to nonlinear feedback control, in: Proc. 15th Mediterranean Conf. on Control and Automation, pp. 1–6.

[20] Mboup, M., Join, C., Fliess, M., 2009. Numerical differentiation with annihilators in noisy environment. Numerical Algorithms 50, 439–467.

[21] Mboup, M., Join, C., Fliess, M., Wang, Y., Zheng, G., Efimov, D., Perruquetti, W., 2020. Comments on 'differentiator application in altitude control for an indoor blimp robot'. Int. J. Control 93, 1218–1219.

[22] Mboup, M., Riachy, S., 2014. A frequency domain interpretation of the algebraic differentiators. IFAC Proc. Volumes 47, 9147–9151.

[23] Mboup, M., Riachy, S., 2018. Frequency-domain analysis and tuning of the algebraic differentiators. Int. J. Control 91, 2073–2081.

[24] Menhour, L., d'Andréa-novel, B., Fliess, M., Mounier, H., 2013. Multivariable decoupled longitudinal and lateral vehicle control: A model-free design, in: Proc. 52nd IEEE Conf. on Decision and Control, pp. 2834–2839.

[25] Olver, F., 1965. On the asymptotic solution of second-order differential equations having an irregular singularity of rank one, with an application to Whittaker functions. J. Soc. Indust. Appl. Math. Ser. B Numer. Anal. 2, 225–243.

[26] Perruquetti, W., Floquet, T., 2007. Homogeneous finite time observer for nonlinear systems with linearizable error dynamics, in: Proc. 46th IEEE Conf. on Decision and Control, pp. 390–395.

[27] Shtessel, Y., Edwards, C., Fridman, L., Levant, A., 2013. Sliding Mode Control and Observation. Control Engineering, Springer New York.

[28] Szegö, G., 1939. Orthogonal Polynomials. AMS.

[29] Vasiljevic, L.K., Khalil, H.K., 2008. Error bounds in differentiation of noisy signals by high-gain observers. Syst. Control. Lett. 57, 856 – 862.

[30] Wang, Y., Zheng, G., Efimov, D., Perruquetti, W., 2018. Differentiator application in altitude control for an indoor blimp robot. Int. J. Control 91, 2121–2130.